



Model-based investigation of electric vehicle battery aging by means of vehicle-to-grid scenario simulations



Clemens Guenther^{a,*}, Benjamin Schott^a, Wilfried Hennings^b, Paul Waldowski^c, Michael A. Danzer^a

^a Zentrum für Sonnenenergie- und Wasserstoff-Forschung Baden-Württemberg (ZSW), Akkumulatoren, Lise-Meitner-Straße 24, 89081 Ulm, Germany

^b Forschungszentrum Jülich GmbH, Institut für Energie- und Klimaforschung, Systemforschung und Technologische Entwicklung, 52425 Jülich, Germany

^c Technische Universität Berlin, Fachgebiet Kraftfahrzeuge, 13355 Berlin, Germany

HIGHLIGHTS

- Model-based investigation of the electric vehicle battery aging.
- Load scenarios depend on driving cycles, charging strategies, and peak-shaving.
- Battery life could be prolonged by time-controlled or demand-driven recharging.
- Simulated life of the modeled battery could endure a usual life of a passenger car.

ARTICLE INFO

Article history:

Received 1 October 2012

Received in revised form

7 December 2012

Accepted 8 February 2013

Available online 26 February 2013

Keywords:

Aging

Battery model

Electric vehicle

Lithium-ion

Vehicle-to-grid

ABSTRACT

Main objective of this work is the model-based investigation of the impact of different load scenarios on the estimated useful life of a traction battery. An energy-based battery model is used for simulation of the available energy of the battery. Reduction of the energy storage capability of the battery is considered by an aging model. The aging model consists of a calendar and a cycle aging model. All models are implemented for simulation of present and future lithium-ion technologies. Hence, the range of battery characteristics and the aging behavior can be varied. In 2020 electric vehicles presumably will have reached a significant number and feed-back of electrical power from the vehicle to the power grid can be expected as an implemented ancillary service. Hence the battery's load scenarios comprise different combinations of driving cycles, charging strategies, and peak-shaving. Therefore the impact of these scenarios on battery aging can be identified by means of the model-based investigation of the battery lifetime. The presented battery model considers aging effects and is a useful tool for the design of an electric vehicle, for the dimensioning of a battery system depending on climate and user behavior, as well as for cost calculations.

© 2013 Elsevier B.V. All rights reserved.

1. Introduction

Nowadays conventional vehicles normally use fossil fuels for their internal combustion engine. The availability of fossil fuels is limited and combustion pollutes the environment. So conventional vehicles are continuously improved and alternatives are examined. These alternatives include biofuels and vehicles with electric drive components. On the one hand, electric vehicles are a challenge for batteries. Therefore safety, specific energy, and specific power of the batteries are improved permanently. On the other hand, the batteries utilization ratio is low because of the long rest periods of private cars.

Simultaneously the integration of renewable energies in power grids is progressing. Additional storage for electric energy is required due to the intermittent energy supply and the additional need for stabilization of the power grid. Synergies of electric vehicles and renewable energies may help to meet these challenges. Possibilities, advantages, and limitations of a vehicle-to-grid (V2G) system are investigated and discussed. Contributions to stability of the power grid could improve the degree of utilization of a battery and potentially generate revenue.

Since the publication of Kempton et al. in 1997 [1], it is under investigation whether a stock of electric vehicles, connected to the grid, can significantly contribute to distributed energy storage. Fundamentals and implementation of a vehicle-to-grid system are studied in Refs. [2,3]. Both plug-in hybrid vehicles (PHEV) and battery electric vehicles (BEV) can be connected to

* Corresponding author. Tel.: +49 731 9530540; fax: +49 731 9530599.

E-mail address: clemens.guenther@zsw-bw.de (C. Guenther).

the power grid for charging of their traction battery. Availability of vehicles for a grid connection is one prerequisite for vehicle-to-grid – bidirectional energy exchange and communication between vehicles and a smart power grid. The US fleet of vehicles is not used for driving more than 95% of a day [1]. Private passenger cars are available more than 89% of one day for grid connection in Germany [4]. In this work it is assumed that the described utilization of cars does not change considerably in the near future.

Today and at least until 2030 lithium-ion batteries will be used to store electrical energy in prototype and commercial electric vehicles (EV). Reasons for that assumption are the higher specific energy, higher specific power and longer lifetime in comparison to other battery technologies [5–8]. Nevertheless, the aging of a traction battery can be accelerated by additional stress, which is caused by ancillary services. The estimation of the useful life of batteries is very important because of their costs and warranty, which has to be extended by the manufacturers. Costs for lithium-ion systems are comparatively high these days. Particularly in long-term applications, like photovoltaic systems or electric mobility, a best possible prediction of the useful life is necessary for a precise cost calculation. The economics of ancillary services are studied in Refs. [9–12]. The sensitivities and optimizations of economics, battery degradation and charging strategies are investigated in Refs. [12–14]. Thus the question, which is addressed in this work, arises: How do different load scenarios, comprising different combinations of driving cycles, charging strategies, and an ancillary service, affect the lifetime of a traction battery in an electric car?

In Ref. [15] the battery aging is studied based on measurements using realistic duty cycles. In Ref. [11] a model-based investigation of the charging and battery degradation costs is presented. The main focus of this report is the battery aging induced by different V2G duty cycles. Therefore a novel approach for modeling battery aging is presented. The energy-based battery model considers the reduction of the energy storage capability due to calendar and cycle aging. In comparison to previous works, here a BEV physics model is used to calculate the battery load and the investigated driving cycles are based on the New European Driving Cycle (NEDC) and two measured real life driving cycles. Furthermore a literature study is carried out, which provides an adaptation of the battery model to the expected future development of battery key parameters. The assumed daily travel behavior corresponds to results of Ref. [16]. The impact of different driving cycles charging strategies and an ancillary service on battery aging is investigated. Thus, conclusions about the useful life of the modeled BEV traction battery are possible.

2. Battery model

Different mathematical model approaches are presented in literature to simulate the electric behavior of a battery. For example on the one hand equivalent circuit models are used for simulation of the battery voltage [17–28] and on the other hand fundamental battery models based on physical and electrochemical equations [29–36] can be used for the description of processes taking place in a battery. An energy-based battery model is used for the scenario simulations in this work. This approach is used according to the advantages that the model parameters can easily be adapted and the runtime of the simulations decrease significantly in comparison to usage of a dynamic equivalent circuit model.

Time dependency of variables is not stated explicitly in Subsections 2.1 and 2.2.

2.1. Energy-based battery model

The available energy content E_B of a traction battery depends on the requested electric power P_B of the EV. By definition the battery is discharged by a negative power and charged by a positive power. The round trip energy efficiency

$$\eta_{Wh} = E_{dc}/E_{ch} \quad (1)$$

is defined by the ratio of the discharged E_{dc} and charged energy E_{ch} . The energy efficiency of lithium-ion batteries is about 95% [37]. The electric power of the battery

$$P_B = P_{los} + P_{eff} \quad (2)$$

is defined as the sum of the power losses P_{los} and the effective power P_{eff} . While the losses heat up the battery, the effective power changes the available energy of the battery. The losses are due to ohmic resistances in the current connectors and in the electrolyte as well as charge transfer and diffusion.

Integration over time of the effective electric power leads to the available energy of the battery

$$E_B = E_0 + \int P_{eff} dt \quad (3)$$

considering the initial value $E_0 = E_B(t_0 = 0)$. The state of charge (SOC) is a time-dependent variable, which notifies the charge amount of a battery in relation to its nominal capacity C_N . Usually the SOC is calculated by an integration of the applied battery current I_B , which is normalized to C_N [37,38]. There is no energy available for SOC = 0 and the available energy reaches its maximum for SOC = 1. In this work the state of energy (SOE) of a battery is defined according to

$$SOE = E_B/SE_N \quad (4)$$

by a normalization of the available energy to the nominal storable energy SE_N .

The scenario simulations in this work are conducted on the assumption that the battery temperature T_B is equal to the ambient temperature, while no current is applied to the traction battery, and is constantly controlled to 35 °C during operation.

2.2. Battery aging model

Aging of a battery is due to electrochemical degradation processes, as described in Refs. [39–42]. The degradation processes take place during operation and also at rest periods where no current is applied. Aging leads to a decreasing capacity and an increasing internal resistance. There exist some other effects like i.e. an increasing self-discharge rate, but they are not considered in this work, because of their comparatively low impact on the question, which is investigated in this work. As a consequence of this, model parameters become time-dependent. Hence, the energy storage capability is reduced by aging. The calendar aging A_{cal} is affected by the potential and the temperature of the battery. The usage of the cell increases the cycle aging A_{cyc} additionally due to current I_B and cycle depth. The assumptions are made, that the calendar aging occurs even during operation and that the total aging of the cell A_B can be expressed by a superposition of calendar and cycle aging

$$A_B = A_{cal} + A_{cyc} \quad (5)$$

The state of health (SOH) is a time-dependent factor, which can be used for the evaluation of the actual state of a battery in

comparison to its state at begin of life (BOL). The state of health of a battery is connected to aging by

$$SOH = 1 - A_B \quad (6)$$

and it decreases over time. It is one at BOL and zero at end of life (EOL). The storable energy SE is reduced by aging as given in

$$SE = SE_N \cdot (0.8 + 0.2 \cdot SOH), \quad (7)$$

where the EOL is fixed by definition to 20% energy loss compared to the initial value at BOL. The state of energy

$$SOE = E_B / SE \quad (8)$$

is then calculated by a normalization of the battery energy E_B to the storable energy SE under nominal conditions.

2.2.1. Calendar aging

The calendar aging of a cell is mainly driven by chemical reactions between the electrolyte and the electrodes, so that the solid electrolyte interphase (SEI) is growing and lithium-ions are lost for the storage of energy [39]. In Refs. [43–46] the calendar aging or the lithium loss, respectively, is proportional to the root of the time. These reactions are influenced by the electrochemical potential and the temperature in the cell. The investigations presented in Refs. [46–48] have shown that the influence of the temperature behaves exponentially according to the Arrhenius equation. The values of the activation energy are specifying that the reaction rate (aging) is doubled, with an increase in temperature by 10–15 K Refs. [49,50]. In Refs. [43,48] different dependencies of the aging rate on the state of charge are shown. Thus, a doubled aging rate is assumed with a temperature rise of 15 K and an increase of the state of charge by 40%. An exponential dependency of the aging on SOE is assumed, analogue to SOC-dependency reported in Refs. [47,49,51]. Therefore, the following approach

$$A_{cal} = A_0 \cdot \exp\left(\frac{SOE - SOE_0}{b}\right) \cdot \exp\left(\frac{T_B - T_0}{c}\right) \cdot \sqrt{t} \quad (9)$$

is assumed for the calendar aging, with the coefficient A_0 corresponding to the nominal lifetime, while the cell is kept at the states SOE_0 and T_0 .

2.2.2. Cycle aging

The cycle aging model, which is used in this work, is based on following assumptions. All cycles which possess an identical cycle depth ΔSOE exhibit an equal impact on cycle aging. Different mean SOE are considered by the calendar aging model implicitly. The aging which is caused by a completed cycle, comprising charging and discharging, could be halved, when only one part of the entire cycle, the charging or discharging, was applied to the battery, on condition that the cycle depth is the same. The aging per cycle a_{cyc} depends nonlinearly on the cycle depth. The assumed dependency of the aging per cycle on the cycle depth is depicted in Fig. 1. While the applied current is not equal to zero, a cubic polynomial

$$a_{cyc} = \begin{cases} \alpha \cdot \Delta SOE^3 + \beta \cdot \Delta SOE^2 + \gamma \cdot \Delta SOE, & I_B \neq 0 \\ 0, & I_B = 0 \end{cases} \quad (11)$$

is used for an approximation of the data. The cycle aging A_{cyc} for the entire considered period is calculated by a summation

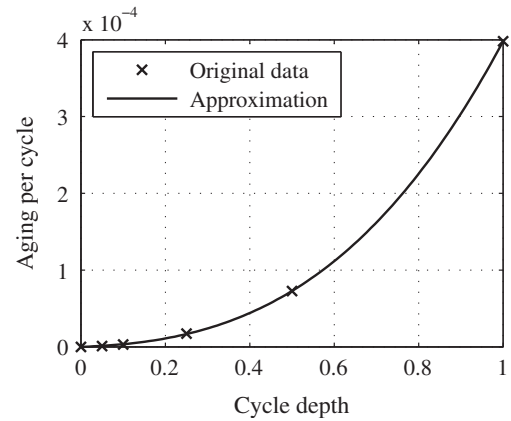


Fig. 1. Assumed aging per cycle a_{cyc} as a function of cycle depth ΔSOE at nominal temperature and a 1 C-rate.

$$A_{cyc} = \sum_{k=0}^N a_{cyc,k}(\Delta SOE_k, I_{B,k}) \quad (12)$$

with the cycle number $k = 0 \dots N$, using the starting value $\Delta SOE_0 = 0$.

The inputs SOE and T_B of the calendar aging model are output variables of the energy-based battery model. The cycle depth ΔSOE is not calculated in the battery model. Hence an algorithm is developed to determine the cycle depth ΔSOE for any SOE curve. The inputs of the battery model for the scenario simulations are synthetically generated. Therefore the SOE curve is not noisy and a simple algorithm can be used to identify the cycle depth. The algorithm detects local extrema of SOE and calculates the difference, the cycle depth, between two successive local extrema. The combination of this algorithm and the aging model expressed by Eqs. (11) and (12) leads to a discontinuous, monotone increasing curve for the cycle aging A_{cyc} when simulating.

2.3. Parameterization

Lithium-ion cells for electronic devices, such as laptops, smart phones or video cameras are already highly developed. The production volume of these cells is about several million units per year. There will be new and different requirements in terms of safety, durability, capacity and performance for new applications in the nearby future, in particular for EVs. The new requirements necessitate further research and development efforts, enabling a continuous improvement of the state of the art. To estimate the future development as well as possible and to set appropriate milestones for development programs, technology roadmaps have been developed by various institutions. Major parameters that are estimated here are the future development of the specific costs, the useful life (calendar and cycle life) as well as the specific power and the specific energy for cells and battery systems. However, the important aspect of security can hardly be presented with measurable variables and therefore is not considered in most roadmaps quantitatively. The parameters of the energy-flow-based battery model, such as energy density, efficiency and life span can be estimated by a literature study of such technology roadmaps. For the comprehensive modeling of future battery systems a sound data base for the cell parameters is necessary.

Based on Refs. [52–62] the future development of key parameters of the battery model, like specific energy and calendar as well as cycle life, can be estimated. Table 1 shows the battery parameters for a future lithium-ion battery as an extract of the above-mentioned literature study for a specified vehicle. The vehicle is a

Table 1

Parameters for the modeled lithium-ion battery, which were assumed to be realistic in 2020.

| Parameter | Value |
|--|-------|
| Energy (kWh) | 21 |
| Used Energy (kWh) | 16.8 |
| Battery weight (kg) | 116 |
| Cell weight (kg) | 93 |
| Weight of components (kg) | 23 |
| Specific battery energy (Wh kg ⁻¹) | 180 |
| Specific cell energy (Wh kg ⁻¹) | 225 |
| Energy efficiency (%) | 96 |
| Calendar life A_{cal} (years) | 12 |
| Cycle life A_{cyc} (cycles) | 2500 |

compact class battery electric vehicle with a range of 120 km in the NEDC [63] as described in subsection 3.1.

3. Scenarios

In this work it is assumed that electric vehicles will have reached a significant number and the feed-back of electrical power to the power grid can be expected as an implemented ancillary service in 2020. A comparison of the aging of an EV battery, as it will assumedly be used in 2020, is carried out relative to different load scenarios by a model-based investigation. The load scenarios are combinations of different driving cycles, charging strategies and an ancillary service.

3.1. Driving cycles

Three different driving cycles are used for the scenario simulations. One is based on the synthetical NEDC. The other two are based on different real life driving cycles, which were recorded by a GPS data logger [64]. The driving cycles used for the scenario simulations should match a variation of the characteristic daily travel behavior of a usual German car driver. A German nationwide survey [16] of 50,000 households on behalf of the Federal Ministry of Transport, Building and Urban Affairs (BMVBS) is analyzed. Only non-corporate drivers are interviewed in this survey. They do about 4 trips per day with an average distance of 11.8 km and 90% of all daily driven distances are below 90.1 km. More than 70% of the interviewed persons own a garage or a parking, 93% of the cars are parked there at night, and never more than 13% of all drivers are on the road at the same time.

The above-mentioned driving profiles are used as a basis for the synthetical generation of a reference driving cycle (RDC), an urban (UDC), and an extra-urban driving cycle (EUDC), which meet the identified German driver behavior. The generation of the driving cycles is done by repeating and scaling parts of the NEDC and the measured real life driving cycles. Some of the characteristics of the generated driving cycles are shown in Table 2. The UDC shows the lowest average speed and shortest trip distance, while the RDC

Table 2

Summary of the main characteristics of the reference driving cycle (RDC), the urban driving cycle (UDC), and the extra-urban driving cycle (EUDC).

| Driving cycle | Data basis | Dynamic | Mean speed (km h ⁻¹) | Power range (kW) | Distance per day (km d ⁻¹) | Distance per year (km a ⁻¹) |
|---------------|------------|----------|----------------------------------|------------------|--|---|
| Reference | NEDC | Moderate | 33.6 | −40–+20 | 32.8 | 11,972 |
| Urban | Real life | High | 17.6 | −80–+40 | 18.3 | 6672 |
| Extra-urban | data | High | 36.5 | −110–+40 | 39.9 | 14,560 |

shows the least energy consumption due to the small power range and the moderate dynamics. The EUDC exhibits the upper limit in all of the shown characteristics.

The demand for electrical power which has to be provided by the traction battery is calculated by a vehicle physics model. The model has been already reported in Ref. [65]. Table 3 shows a summary of some important model parameters for a battery electric compact car in 2020.

3.2. Charging strategies and grid services

For the definition of the charging strategies it is assumed, that all BEV owners are able to charge their traction batteries at home and they use this charging station only. The charging strategies and their influence on battery aging differ in the starting time, the applied constant power, and the duration. The starting time of the charging procedures is varied for the simulation of a user-driven as well as a time-controlled charging. In the user-driven strategy charging starts 5 min after arrival at home and not later than 5 pm. The time-controlled strategy simulates charging in periods of low demand for electricity. The duration of the charging periods results from the combination of a specific charging strategy with the energy consumption of a specific driving cycle. The electrical power ratings, which are used during the charging processes, are due to the one-phase (3.3 kW) and the three-phase (9.9 kW) alternating current building connections. The charging times in the scenarios 7–9 vary due to the simulated peak-shaving between November and February from 5 pm to 7 pm.

For any driving profile shown in Table 4 the last trip ends before 5 pm. Hence, in the user-driven charging strategy the charging starts at 5 pm because it is assumed that the driver arrives at home until 5 pm and starts charging right after coming home. The starting time of the second charging strategy is set to midnight and simulates the time-controlled charging which is referred to the attempt to counteract the low demand for electricity at night. In the scenarios 7–9 a higher power is used and it is assumed that electrical power is discharged from the battery to the power grid between November and February from 5 pm until 7 pm to level out the higher demand for electricity in this period.

The nine scenarios in Table 4 are supplemented by other variants that are not listed in the table. In the scenarios, which are indicated by the index b (for example, scenario 4b), the traction battery is recharged every other day. This variant exists only for those scenarios, in which the energy consumption of the applied driving cycle could be provided by the battery for two days. For the scenarios 7–9 exist reference scenarios without grid service, indicated by the index c (for example, scenario 7c), to identify the impact of the grid service.

In spite of the values of charging power and charging time given in Table 4, the power may set to zero in the battery model in order to avoid overcharge or deep discharge.

Table 3

Parameters of a battery electric compact car in 2020.

| Parameter | Value |
|---|--------------|
| Drag coefficient times area (m ²) | 0.293 · 2.25 |
| Rolling resistance coefficient (10 ⁻³) | 7.48 |
| Auxiliary consumers (W) | 1500 |
| Electrical range in NEDC (km) | 120 |
| Total weight (kg) | 1265 |
| Energy consumption in NEDC (kWh 100 km ⁻¹) | 15.54 |
| Efficiency electric motor plus power electronics (%) | 88 |
| Efficiency of power transfer from regenerative braking to batteries (%) | 85 |

Table 4
Basic points for the simulated scenarios, which are built up of combinations of the driving cycles, the charging strategies and a feed-back of electrical power to the grid.

| Scenario | Driving cycle | Charging strategy | Starting time | Charging power (kW) | Feed-back power (kW) | Charging time (h:mm) | |
|----------|---------------|-------------------|---------------|---------------------|----------------------|----------------------|-----------|
| | | | | | | Mar.–Oct. | Nov.–Feb. |
| 1 | RDC | User-driven | 5 pm | 3.3 | 0.0 | 1:44 | |
| 2 | UDC | User-driven | 5 pm | 3.3 | 0.0 | 1:07 | |
| 3 | EUDC | User-driven | 5 pm | 3.3 | 0.0 | 2:44 | |
| 4 | RDC | Time-controlled | 12 pm | 3.3 | 0.0 | 1:44 | |
| 5 | UDC | Time-controlled | 12 pm | 3.3 | 0.0 | 1:07 | |
| 6 | EUDC | Time-controlled | 12 pm | 3.3 | 0.0 | 2:44 | |
| 7 | RDC | Time-controlled | 12 pm | 9.9 | 5.3 | 0:34 | 1:42 |
| 8 | UDC | Time-controlled | 12 pm | 9.9 | 5.9 | 0:22 | 1:37 |
| 9 | EUDC | Time-controlled | 12 pm | 9.9 | 3.0 | 0:54 | 1:33 |

3.3. Daily duty cycles

The daily duty cycles of the investigated scenarios are created by different combinations of driving cycles, charging strategies, and one ancillary service. Table 4 summarizes the basic points for all combinations of the different driving cycles and charging strategies. During the scenario simulations, the daily duty cycles are repeated until the end of the useful life of the modeled BEV traction battery. As an example for the load cycles, Fig. 2 shows the electrical power, which has to be provided by the battery, in scenario 7. In this case, the load cycle is a combination of the NEDC-based reference driving cycle, peak-shaving, and recharging.

3.4. Ambient temperature

For the scenario simulations an annual variation of the ambient temperature for a particular location is needed. An algorithm is applied for the calculation of a characteristic daily variation of the ambient temperature. The calculation is based on the minimum and maximum values of the temperature and their probabilities of occurrence. In this work the averaged temperature data for the location of Berlin of the past decade are used to generate the annual variation of the ambient temperature. Like shown in Fig. 3, the minimum ambient temperature is slightly above -5°C and the maximum is approximately 28°C .

4. Results and discussion

Due to the high costs of the batteries for energy storage for the propulsion of electric vehicles, there is particular interest in both information about the current state of the battery and its future

development. In the presented results the previously defined state of health specifies the energy storage capability. The simulation results of a selection of the above-defined scenarios are presented and discussed in the following paragraphs.

According to the scenarios 1–3, the user-driven charging strategy is combined with three different driving cycles to estimate the influence of the driving cycles on the aging behavior of the battery. Fig. 4 shows the simulated *SOH* as a function of time for the scenarios 1–3. For the scenarios 1 and 2, which are based on the RDC and the UDC, battery lifetimes of 10.35 years and 10.65 years are achieved. However, the third scenario shown in Fig. 4 leads to a useful life of about nine years. Three factors come into consideration as a reason for this significant difference between the several results – the state of charge, the temperature and the cycle depth. In the measured extra-urban driving cycle, the most energy is consumed. Therefore the longest durations of the charging periods can be found in Table 4 for all scenarios, which use this driving profile. At least for the recharging, scenario 3 exhibits the largest cycle depth in comparison with the other driving cycles (scenarios 1 and 2). After the first simulated day, the cycle aging in scenario 3 is about twice as large as in the other two scenarios. Due to the high quota of standstill on the one hand and the methods used in the aging model on the other hand, the calendar aging has a dominant influence on the lifetime of the battery in comparison with the cycle aging. In scenario 3, the percentage of the calendar aging is 99.96% in reference to the total aging after one day. This calendar aging percentage is qualitatively representative for all those scenarios. A comparison of the mean values of the cells *SOE* and temperature, which were averaged over the first day of the scenario simulations, is used to find an indication of the reason for the differences in the calendar aging. The average *SOE* decreases from scenario 1 to scenario 3. The influence of the state of energy or rather the voltage on the calendar aging is best in the case of

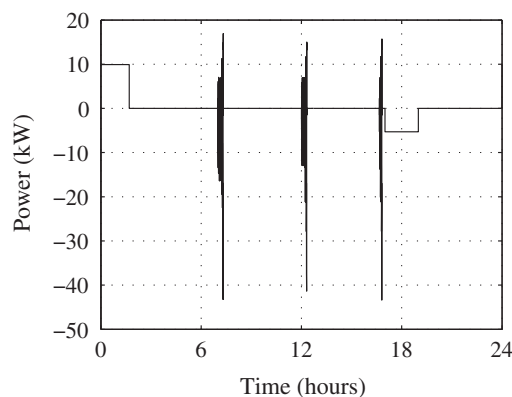


Fig. 2. Electrical power of scenario 7 for one day between November and February is a combination of the reference driving cycle, peak-shaving from 5 to 7 pm, and recharging starting at midnight.

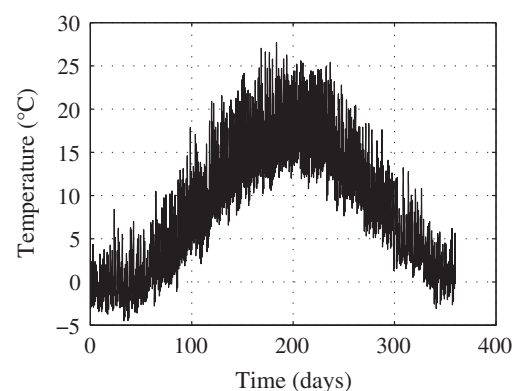


Fig. 3. Ambient temperature generated for the location of Berlin.

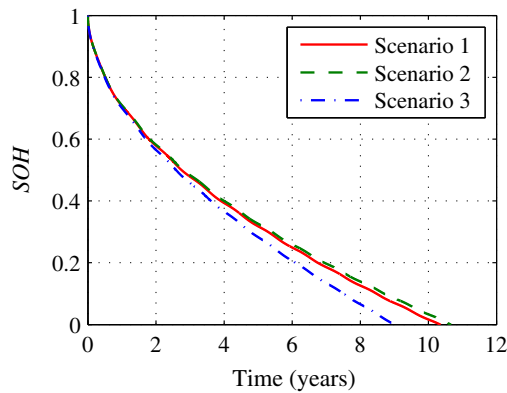


Fig. 4. State of health as a function of time for the user-driven charging strategy in combination with different driving cycles.

scenario 3 and thus can not be the reason for the comparatively rapid aging. However, the mean temperature (4.84°C) of scenario 3 is higher than in scenarios 1 (2.76°C) and 2 (2.70°C). The longer travel times are the reason for the higher values, because then the temperature of the cell (35°C) is well above the ambient temperature. Due to the exponential impact of the cell temperature on the calendar aging, the temperature obviously is the second reason for the shorter battery life in scenario 3.

In Fig. 5 the time-dependent profiles of the SOH are depicted for the combination of the NEDC-based reference driving cycle with three different charging strategies. Scenario 1 leads to shortest useful life of a little more than ten years. In comparison to scenario 4 the battery is recharged a few hours earlier every day. This leads to a higher average SOE and therefore to a shortening of the useful life by almost one year. Since the energy consumption in this driving cycle is comparatively low, this load profile can be applied two days in a row without recharging. This power profile is referred to scenario 4b and leads to the longest lifetime in Fig. 5 with approximately 13 years. In scenario 1 the battery spends more time of their useful life at higher states of charge and thus at higher stress levels than in the scenarios 4 and 4b. The higher voltage due to this higher SOE is the reason for the accelerated aging.

For the investigation of the influence on the battery aging caused by the energy feed-back to the EV to the power grid the simulation results of scenarios 7 and 7c are compared. Some basic data of the simulation results are summarized in Table 5. Scenario 7 leads to a reduction in battery life of approximately three years due to longer operating times and larger cycle depths. The traveled

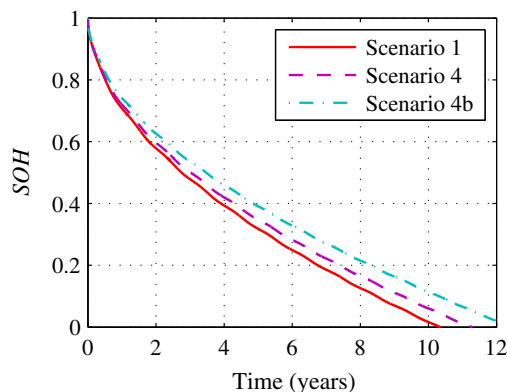


Fig. 5. State of health as a function of time for different charging strategies using the reference driving cycle.

Table 5

Lifetime, driven distance, and energy throughput of two NEDC-based scenarios, scenario 7 contains ancillary services and scenario 7c does not.

| Scenario | Lifetime (years) | Driven distance (km) | Energy throughput (MWh) |
|----------|------------------|----------------------|-------------------------|
| 7 | 8.7 | 104,550 | 72.8 |
| 7c | 11.8 | 141,270 | 44.8 |

distance is reduced by about 36.10^3 km. However, the total energy throughput increases by more than 60% to approximately 73 MWh. About 33 MWh of the energy throughput originate from driving and the according recharging. There are approximately 20 MWh electrical energy feed-back to relieve the power grid from November to February between 5 pm and 7 pm for almost 8.7 years.

5. Conclusions

In this work a battery model with consideration of aging effects is presented. A model-based investigation of battery aging is discussed for different EV load profiles by means of scenario simulations. Battery aging is compared for different scenarios, comprising different combinations of driving cycles, charging strategies, and an ancillary service. The influence of load parameters – like daily distance or starting time of charging – on aging is shown.

The main results of the scenario simulations are the extension of battery life by time-controlled charging (time shift of charging from begin of a standstill to a subsequent time) as well as by demand-driven charging of the vehicle battery (delay of charging until the amount of the remaining energy is inadequately for the next planned trip), estimated life of the modeled high-voltage traction batteries ranges approximately from 8.5 years to 13 years and the simulated peak-shaving reduces the battery life due to additional cycling and leads to an increase of the specific costs.

The presented battery model considers aging effects and is a useful tool for the design of electric vehicles, for the dimensioning of a battery system depending on climate and user behavior, and for aging-dependent cost calculations of batteries.

Acknowledgement

The authors gratefully acknowledge the very good collaboration with all project partners. Special thanks to Jochen Linssen, who is with Forschungszentrum Jülich GmbH, for exemplary managing the consortium.

This work was funded by the Federal Ministry of Economics and Technology, following a decision of the German Bundestag. The responsibility for the content of this publication lies with the authors.

References

- [1] W. Kempton, S.E. Letendre, *Transport. Res. D-Tr.* E 2 (1997) 157.
- [2] W. Kempton, J. Tomiá, *J. Power Sources* 144 (2005) 268.
- [3] W. Kempton, J. Tomiá, *J. Power Sources* 144 (2005) 280.
- [4] N. Hartmann, E.D. Özdemir, *J. Power Sources* 196 (2011) 2311.
- [5] T. Markel, A. Simpson, in: *Proceedings of the Advanced Automotive Battery Conference 2006*, pp. 1033–1039.
- [6] A.F. Burke, *Proc. IEEE* 95 (2007) 806.
- [7] M. Anderman, in: *Proceedings of the Large Lithium Ion Battery Technology and Application Symposium*, Long Beach, California, USA, 2009.
- [8] B. Scrosati, J. Garche, *J. Power Sources* 195 (2010) 2419.
- [9] S.B. Peterson, J.F. Whitacre, *J. Apt. J. Power Sources* 195 (2010) 2377.
- [10] C.D. White, K.M. Zhang, *J. Power Sources* 196 (2011) 3972.
- [11] B. Lunz, Z. Yan, J.B. Gerschler, D.U. Sauer, *Energy Policy* (2012).
- [12] E. Sortomme, M.A. El-Sharkawi, *IEEE Trans. Smart Grid* 3 (2012) 351.
- [13] S. Bashash, S.J. Moura, J.C. Forman, H.K. Fathy, *J. Power Sources* 196 (2011) 541.
- [14] J. Neubauer, A. Brooker, E. Wood, *J. Power Sources* 209 (2012) 269.
- [15] S.B. Peterson, J. Apt, J.F. Whitacre, *J. Power Sources* 195 (2010) 2385.

- [16] Mobilität in Deutschland 2008, Mobility in Germany (2008). [Online]. Available: http://www.mobilitaet-in-deutschland.de/02_MiD2008/publikationen.htm [accessed 23.11.12.].
- [17] E. Barsoukov, J.H. Kim, C.O. Yoon, H. Lee, J. Power Sources 83 (1999) 61.
- [18] L. Gao, S. Liu, R.A. Dougal, IEEE Trans. Compon. Pack. Technol. 25 (2002) 495.
- [19] B.Y. Liaw, G. Nagasubramanian, R.G. Jungst, D.H. Dougherty, Solid State Ionics 175 (2004) 835.
- [20] S. Buller, M. Thele, R.W.A.A. DeDoncker, E. Karden, IEEE Trans. Ind. Appl. 41 (2005) 742.
- [21] M. Chen, G.A. Rincon-Mora, IEEE Trans. Energy Conver. 21 (2006) 504.
- [22] J.B. Gerschler, J. Kowal, M. Sander, D.U. Sauer, in: Proceedings of the Electric Vehicle Symposium (EVS 23), 2007, Anaheim.
- [23] R.C. Kroeze, P.T. Krein, in: Proceedings of the Power Electronics Specialists Conference, 2008. (PESC 2008), IEEE, Rhodes, Greece, 2008, pp. 1336–1342.
- [24] M.A. Roscher, J. Vetter, D.U. Sauer, J. Power Sources 191 (2009) 582.
- [25] J.B. Gerschler, F.N. Kirchhoff, H. Witzenhause, F.E. Hust, D.U. Sauer, in: Proceedings of the 5th International IEEE Vehicle Power and Propulsion Conference, IEEE, Dearborn, Michigan, USA, 2009, pp. 295–303.
- [26] Y. Hu, S. Yurkovich, Y. Guezennec, B.J. Yurkovich, J. Power Sources 196 (2011) 449.
- [27] J. Remmlinger, M. Buchholz, M. Meiler, P. Bernreuter, K. Dietmayer, J. Power Sources 196 (2011) 5357.
- [28] J.P. Schmidt, T. Chrobak, M. Ender, J. Illig, D. Klotz, E. Ivers-Tiffée, J. Power Sources 196 (2011) 5342.
- [29] T.F. Fuller, M. Doyle, J. Newman, J. Electrochem. Soc. 141 (1994) 1.
- [30] M. Doyle, J.P. Meyers, J. Newman, J. Electrochem. Soc. 147 (2000) 99.
- [31] V.R. Subramanian, H.J. Ploehn, R.E. White, J. Electrochem. Soc. 147 (2000) 2868.
- [32] J. Christensen, J. Newman, J. Electrochem. Soc. 151 (2004) A1977.
- [33] G.K. Singh, M.Z. Bazant, G. Ceder, Anisotropic Surface Reaction Limited Phase Transformation Dynamics in LiFePO₄. ArXiv e-prints owned and operated by Cornell University (Jul-2007). [Online]. Available: <http://arxiv.org/abs/0707.1858v1> [accessed 03.08.12.].
- [34] S.G. Stewart, V. Srinivasan, J. Newman, J. Electrochem. Soc. 155 (2008) A664.
- [35] J. Kowal, D. Schulte, D.U. Sauer, E. Karden, J. Power Sources 191 (2009) 42.
- [36] A. Latz, J. Zausch, J. Power Sources 196 (2011) 3296.
- [37] A. Jossen, W. Weydanz, Moderne Akkumulatoren Richtig Einsetzen, vol. 1, Aufl., Reichardt, Untermeitingen, 2006.
- [38] D.U. Sauer, O. Böhlen, T. Sanders, W. Waag, R. Schmidt, J.B. Gerschler, in: M. Schöllmann (Ed.), Proceedings of the Energiemanagement Und Bordnetze II: Innovative Ansätze Für Modernes Energiemanagement Und Zuverlässige Bordnetzarchitekturen, expert-Verl., Renningen, Germany, 2007.
- [39] M. Broussely, S. Herreyre, P. Biensan, P. Kaszlejna, K. Nechev, R. Staniewicz, J. Power Sources 97–98 (2001) 13.
- [40] M. Wohlfahrt-Mehrens, C. Vogler, J. Garche, J. Power Sources 127 (2004) 58.
- [41] M. Broussely, P. Biensan, F. Bonhomme, P. Blanchard, S. Herreyre, K. Nechev, R.J. Staniewicz, J. Power Sources 146 (2005) 90.
- [42] J. Vetter, P. Novák, M.R. Wagner, C. Veit, K.-C. Möller, J.O. Besenhard, M. Winter, M. Wohlfahrt-Mehrens, C. Vogler, A. Hammouche, J. Power Sources 147 (2005) 269.
- [43] I. Bloom, B.W. Cole, J.J. Sohn, S.A. Jones, E.G. Polzin, V.S. Battaglia, G.L. Henriksen, C. Motloch, R. Richardson, T. Unkelhaeuser, D. Ingersoll, H.L. Case, J. Power Sources 101 (2001) 238.
- [44] E.V. Thomas, I. Bloom, J.P. Christophersen, V.S. Battaglia, J. Power Sources 184 (2008) 312.
- [45] T. Yoshida, M. Takahashi, S. Morikawa, C. Ihara, H. Katsukawa, T. Shiratsuchi, J. Yamaki, J. Electrochem. Soc. 153 (2006) A576.
- [46] H.J. Ploehn, P. Ramadass, R.E. White, J. Electrochem. Soc. 151 (2004) A456.
- [47] R.B. Wright, C.G. Motloch, J.R. Belt, J.P. Christophersen, C.D. Ho, R.A. Richardson, I. Bloom, S.A. Jones, V.S. Battaglia, G.L. Henriksen, T. Unkelhaeuser, D. Ingersoll, H.L. Case, S.A. Rogers, R.A. Sutula, J. Power Sources 110 (2002) 445.
- [48] B.Y. Liaw, E.P. Roth, R.G. Jungst, G. Nagasubramanian, H.L. Case, D.H. Dougherty, J. Power Sources 119–121 (2003) 874.
- [49] A. Millner, in: Proceedings of the Conference on Innovative Technologies for an Efficient and Reliable Electricity Supply (CITRES), IEEE, Waltham, MA, USA, 2010, pp. 349–356.
- [50] J. Kümpers, in: Proceedings of the 3rd Technical Conference Advanced Battery Power, Aachen, Germany, 2011.
- [51] O. Erdinc, B. Vural, M. Uzunoglu, in: Proceedings of the IEEE, 2009, pp. 383–386.
- [52] Electrochemical Energy Storage Technical Team – Technology Development Roadmap, U.S. Department of Energy, Energy Efficiency and Renewable Energy, 07-Dec. [Online]. Available: http://www1.eere.energy.gov/vehiclesandfuels/pdfs/program/electrochemical_energy_storage_roadmap.pdf [accessed 17.09.12.].
- [53] Recommendations for the Future of Next-generation Vehicle Batteries, Ministry of Economy, Trade and Industry Japan (METI), Aug-2006. [Online]. Available: <http://www.meti.go.jp/english/information/downloadfiles/PressRelease/060828VehicleBatteries.pdf> [accessed 17.09.12.].
- [54] Cool Earth-innovative Energy Technology Program, Ministry of Economy, Trade and Industry Japan, Mar-2008. [Online]. Available: www.meti.go.jp/english/newtopics/data/pdf/031320CoolEarth.pdf [accessed 17.09.12.].
- [55] D. Howell, J. Barnes, G. Henriksen, V. Srinivasan, J. Deppe, P. Kumar, in: Proceedings of the International Battery, Hybrid and Fuel Cell Electric Vehicle Symposium (EVS24), Stavanger, Norway, 2009.
- [56] Technology Roadmap – Electric and Plug-in Hybrid Electric Vehicles, International Energy Agency, 2009. [Online]. Available: http://www.iea.org/papers/2009/EV_PHEV_Roadmap.pdf [accessed 17.09.12.].
- [57] H. Kobayashi, in: Proceedings of the 50th Battery Symposium Japan, Rechargeable Batteries as Innovative, Energy Storage Devices (2009), Japan.
- [58] L. Holmquist, A. Coda, R&D Priorities for the Greening of Vehicles and Road Transport – A Contribution by CLEPA and EUCAR to the European Green Car Initiative (2009).
- [59] G. Meyer, Milestones of a European Battery Roadmap, European Technology Platform on Smart Systems Integration (EPoSS), Sep-2009. [Online]. Available: <http://www.smart-systems-integration.org/public/electric-vehicle/battery-workshop-documents/presentations/Gereon%20Meyer%20VDIVDE-IT.pdf> [accessed 17.09.12.].
- [60] G. Meyer, Report on the Joint EC/EPoSS/ERTRAC Expert Workshop 2009 – Batteries and Storage Systems for the Fully Electric Vehicle, European Green Cars Initiative, 25-Sep. [Online]. Available: http://www.green-cars-initiative.eu/workshops/Report_WS_Batteries.pdf [accessed 17.09.12.].
- [61] G. Meyer, European Roadmap Electrification of Road Transport, Community Research and Development Information Service of the European Commission, 30-Oct. [Online]. Available: ftp://ftp.cordis.europa.eu/pub/technology-platforms/docs/roadmap-electrification-nov2010_en.pdf [accessed 17.09.12.].
- [62] USABC Goals for Advanced Batteries for EVs, United States Council for Automotive Research LLC (USCAR), 2010. [Online]. Available: http://www.uscar.org/commands/files_download.php?files_id=27 [accessed 18.09.12.].
- [63] Council Directive of 20 March 1970 on the Approximation of the Laws of the Member States on Measures to Be Taken against Air Pollution by Emissions from Motor Vehicles (70/220/EEC), Eur-Lex – Access to European Union Law (20-Mar-1970). [Online]. Available: <http://eur-lex.europa.eu/LexUriServ/LexUriServ.do?uri=CONSLEG:1970L0220:20070101:EN:PDF> [accessed 24.06.12.].
- [64] F. Schüppel, S. Marker, P. Waldowski, V. Schindler, in: Proceedings of the 14th International Forum on Advanced Microsystems for Automotive Applications (AMAA 2010), Berlin, 2010.
- [65] P. Waldowski, S. Marker, A. Schulz, V. Schindler, in: Proceedings of the International Scientific Conference on Hybrid and Electric Vehicles RHEVE 2011, Paris, France, 2011.